European Journal of Immunology

Abrogation of ICOS/ICOS ligand costimulation in NOD mice results in autoimmune deviation toward the neuromuscular system

Nicolas Prevot[1,2], Claire Briet[1,2], Hans Lassmann[3], Isabelle Tardivel[2], Edwige Roy[4], Joëlle Morin[2], Tak W. Mak[5], Anna Tafuri[4] and Christian Boitard[1,2]

[1] INSERM U986, Hôpital Cochin/St Vincent de Paul, Paris, France
[2] Université Paris Descartes, Paris, France
[3] Center for Brain Research, Medical University of Vienna, Vienna, Austria
[4] Institut National de la Santé et de la Recherche médicale, Paris, France
[5] Departments of Medical Biophysics and Immunology, Ontario Cancer Institute, University of Toronto, Toronto, Canada

NOD mice spontaneously develop insulin-dependent diabetes around 10–40 wk of age. Numerous immune gene variants contribute to the autoimmune process. However, genes that direct the autoimmune response toward β cells remain ill defined. In this study, we provide evidence that the *Icos* and *Icosl* genes contribute to the diabetes process. Protection from diabetes in ICOS$^{-/-}$ and ICOSL$^{-/-}$ NOD mice was unexpectedly associated with the development of an autoimmune disorder of the neuro-muscular system, characterized by myositis, sensory ganglionitis and, to a reduced extent, inflammatory infiltrates in the CNS. This syndrome was reproduced upon adoptive transfer of CD4$^+$ and CD8$^+$ T cells from diseased donors to naïve NOD.*scid* recipients. Our data further show that protection from diabetes results from defective activation of autoimmune diabetogenic effector T cells in ICOS$^{-/-}$ NOD mice, whereas acceleration of diabetes in BDC2.5 ICOS$^{-/-}$ NOD mice is induced by a dominant defect in Treg. Taken together, our findings indicate that costimulation signals play a key role in regulating immune tolerance in peripheral tissues and that the ICOS/ICOSL costimulatory pathway influences the balance between Treg and diabetogenic effector T cells.

Key words: Autoimmunity · Costimulation · ICOS · ICOS ligand · Type 1 diabetes

Supporting Information available online

Introduction

Type 1 diabetes (T1D) is an autoimmune disease characterized by the activation of autoreactive lymphocytes against pancreatic β-cell antigens. Mechanisms that initiate the failure of immune tolerance to β cells remain elusive in common forms of T1D. The disease develops as a multifactorial process in which environmental factors concur with a highly multigenic susceptibility background [1]. However, genes that direct the autoimmune response toward β cells remain ill defined.

In animal models such as the NOD mouse, the predominant role of T lymphocytes is supported by experiments in which T1D

Correspondence: Professor Christian Boitard
e-mail: Christian.boitard@htd.aphp.fr

is transferred into naïve recipients by T lymphocytes from diabetic or prediabetic animals. Moreover, T1D is prevented by injection of Ab that interfere with T-lymphocyte activation and fails to develop in diabetes-prone mice in which key genes in T-lymphocyte differentiation or activation are nonfunctional [2]. Both $CD4^+$ and $CD8^+$ T cells are involved [3–5].

The activation of autoreactive T lymphocytes in T1D requires the recognition of autoantigens expressed by β cells as well as costimulatory signals. Membrane proteins of the CD28 gene family mediate major costimulatory signals through their interaction with members of the B7 family expressed on APC and stromal cells. CD28 [6, 7], CTLA4 [8], and ICOS [9, 10] are related proteins of the CD28 family that are encoded by genes clustered within a 300 kb region located on chromosome 2. Gene variants within this region have been associated with susceptibility to T1D [11, 12]. *In vivo* deletion of the *Cd28* or *B7* genes, pharmacological blockade of the CD28 or B7 molecules using monoclonal Ab [13–15], and anti-CTLA4 treatment or the expression of a CTLA4-Ig transgene have all shown to profoundly affect the development of T1D in the NOD mouse [16, 17]. The role of the ICOS/ICOS ligand (ICOSL) costimulatory pathway in the pathogenesis of T1D is still controversial. On the one hand, blockade [18, 19] or *in vivo* deletion [20] of ICOS inhibits the development of T1D in NOD mice; on the other hand, treatment with an ICOS-blocking Ab induces acute T1D in transgenic BDC2.5 NOD mice [21].

To better understand the role of the ICOS/ICOSL costimulatory pathway in the development of T1D, we used a genetic approach, introgressing the *Icos* and *Icosl* null mutations [22] onto the NOD background. We confirm the key role of the ICOS/ICOSL costimulatory pathway in the activation of Treg and diabetogenic effector T cells (T_{eff} cells) in the NOD mouse. However, $ICOS^{-/-}$ or $ICOSL^{-/-}$ NOD mice, while protected from T1D, develop an autoimmune disease that affects neural and muscular cells, indicating that local T-cell interaction within the islet environment is a key factor in immune tolerance.

Results

Abrogation of the ICOS/ICOSL costimulatory pathway protects NOD mice from diabetes

To define the role of ICOS/ICOSL costimulation in T1D development, we studied $ICOS^{-/-}$ and $ICOSL^{-/-}$ NOD mice. The spontaneous incidence of T1D was significantly reduced in female $ICOS^{-/-}$ NOD mice (Fig. 1A) since only 16.6% of them became diabetic by 40 wk of age, as compared with 63.6% for female $ICOS^{+/+}$ NOD mice by 40 wk of age. Since the *Icos* locus (1C2) is located in proximity of other immuno-modulatory genes, including CD28 and CTLA-4, we analyzed mice deficient for *Icosl*, which lies in a completely different genetic region. Female $ICOSL^{-/-}$ NOD mice were protected from T1D to a similar extent as female $ICOS^{-/-}$ NOD mice (Fig. 1A). At 40 wk of age, none of them became diabetic, whereas 57.5% female $ICOSL^{+/+}$ NOD

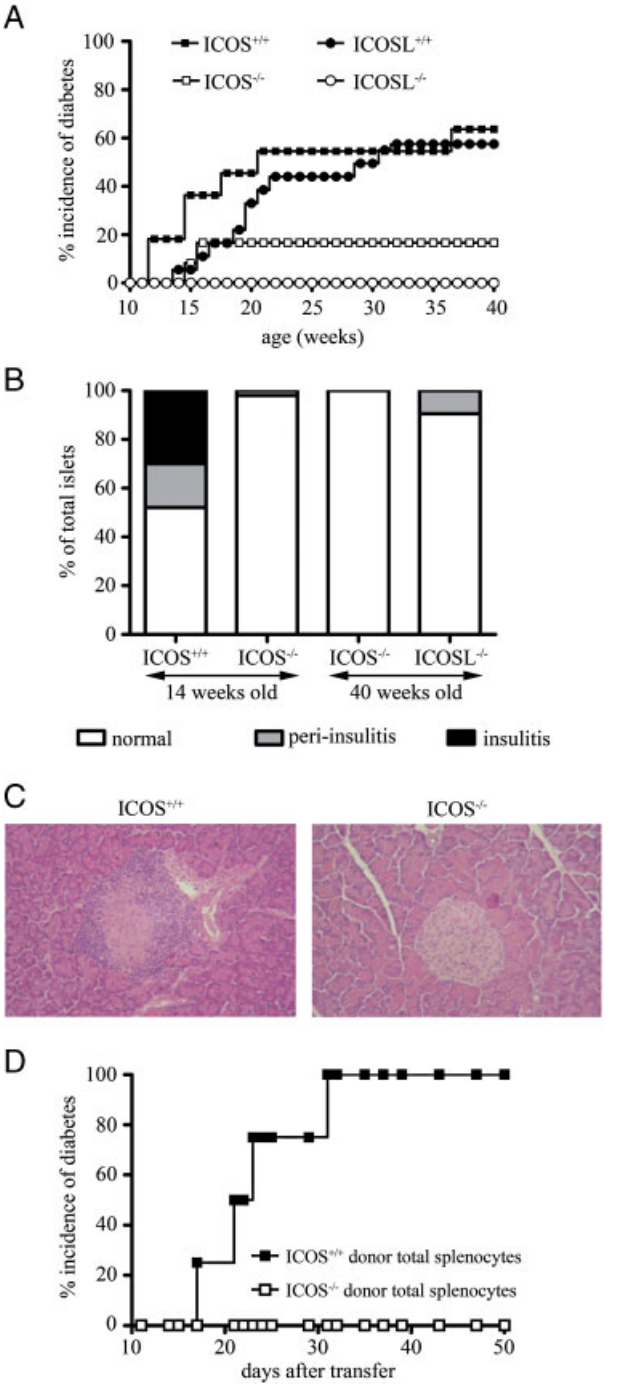

Figure 1. $ICOS^{-/-}$ and $ICOSL^{-/-}$ NOD mice are protected from T1D. (A) Spontaneous incidence of T1D in female $ICOS^{+/+}$ (■, $n = 11$), $ICOS^{-/-}$ (□, $n = 12$), $ICOSL^{+/+}$ (●, $n = 18$), $ICOSL^{-/-}$ (○, $n = 15$) NOD mice. $^*p<0.05$ (Logrank Test). (B) $ICOS^{-/-}$ and $ICOSL^{-/-}$ NOD mice are almost free from insulitis. Percentage of normal islets, peri-insulitis, and insulitis in 14-wk-old female $ICOS^{+/+}$ ($n = 10$ mice) or $ICOS^{-/-}$ ($n = 9$) NOD mice, and in 40-wk-old female $ICOS^{-/-}$ ($n = 6$) or $ICOSL^{-/-}$ ($n = 6$) NOD mice. (C) Representative sections of pancreases from 14-wk-old female $ICOS^{+/+}$ or $ICOS^{-/-}$ NOD mice. (D) Splenocytes from 40-wk-old $ICOS^{-/-}$ NOD mice do not transfer T1D. Briefly, 8-wk-old NOD.*scid* mice were transferred with 10×10^6 stimulated splenocytes from 40-wk-old $ICOS^{-/-}$ (□ $ICOS^{-/-}$ donor total splenocytes, $n = 4$) or $ICOS^{+/+}$ (■ $ICOS^{+/+}$ donor total splenocytes, $n = 4$) NOD mice. $^{**}p<0.01$ (Logrank Test). Data are representative of three independent experiments.

mice developed T1D. Interestingly, both female ICOS$^{-/-}$ and ICOSL$^{-/-}$ NOD mice were also protected from insulitis. At 14 wk of age, 48% of islets from ICOS$^{+/+}$ mice were infiltrated, with 30% of the islets showing invasive insulitis, whereas only 2% islets were infiltrated in ICOS$^{-/-}$ mice (Fig. 1B and C). At 40 wk of age, ICOS$^{-/-}$ NOD mice were free from insulitis, whereas 9.5% of the islets from ICOSL$^{-/-}$ NOD mice showed peri-insulitis (Fig. 1B). In the light of these findings, we next investigated whether the inability to induce T1D was intrinsic to spleen cells from ICOS$^{-/-}$ NOD mice. To this end, splenocytes from 40-wk-old ICOS$^{-/-}$ or ICOS$^{+/+}$ mice were activated *in vitro* by anti-CD3 and anti-CD28 Ab and then adoptively transferred to NOD.*scid* recipients (Fig. 1D). None of the recipient mice transferred with splenocytes from ICOS$^{-/-}$ NOD mice developed T1D upon transfer within a 90-day time frame. By contrast, all recipient mice transferred with splenocytes from control ICOS$^{+/+}$ NOD mice became diabetic within 30 days following transfer (Fig. 1D). Interestingly, both ICOS$^{-/-}$ and ICOSL$^{-/-}$ NOD mice were resistant to the induction of T1D by cyclophosphamide at 8 wk of age (data not shown). Taken together, these observations demonstrate that the ICOS/ICOSL pathway is critical in the early steps leading to failure of immune tolerance to β cells.

ICOS expression during the T1D development

To better understand how the ICOS/ICOSL costimulatory pathway may interfere with the diabetogenic process, we studied ICOS expression during T1D development. We found that ICOS expression was the highest in the islet cell infiltrate (Fig. 2A). In total, 29.2% of CD4$^+$ islet-infiltrating T cells expressed ICOS at 8 wk of age, as compared with 7% in pancreatic LN (PLN), 7.5% in axillary LN (ALN), and 9.2% in the spleen. No significant peak of ICOS expression was seen on CD4$^+$ T cells at earlier stages of the NOD autoimmune process, especially in PLN, although ICOS expression was slightly increasing with age (*i.e.* at 3, 5, and 8 wk of age; Fig. 2B). Since ICOSL can be expressed by various tissues under inflammatory conditions, we studied ICOSL expression in the pancreas. Although ICOSL was expressed, as expected, on infiltrating B cells and APC (data not shown), we observed no ICOSL expression on β cells using flow cytometric analysis (Fig. 2C).

Abrogation of ICOS/ICOSL costimulatory pathway induces acute diabetes in BDC2.5 NOD mice

Several lines of evidence point toward an important role of the ICOS/ICOSL pathway in the differentiation of Treg, including the observation that anti-ICOS monoclonal Ab treatment accelerates the development of T1D in BDC2.5 NOD mice [21]. Since it is difficult to evaluate the level of saturation and accessibility of target cells in studies using blocking Ab, we sought to evaluate the role of ICOS in the development of T1D of BDC2.5 ICOS$^{-/-}$ NOD mice. We observed an increased prevalence of spontaneous

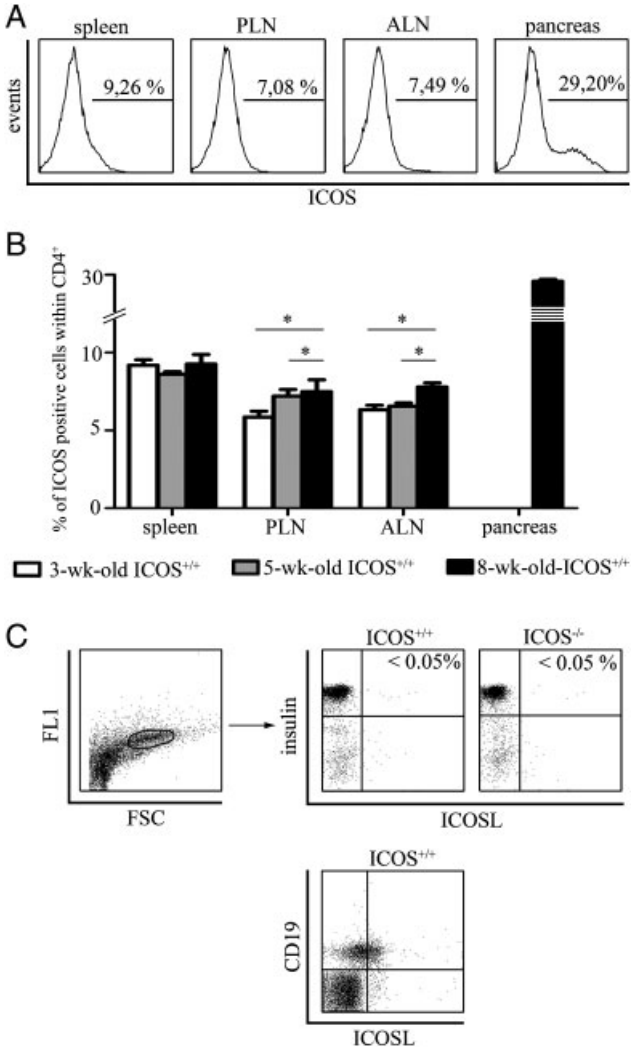

Figure 2. ICOS is strongly expressed on islet-infiltrating CD4$^+$ T cells. (A) ICOS expression on islet-infiltrating T cells. Flow cytometric analysis of ICOS expression on unmanipulated T cells from spleen, PLN, ALN, pancreas of 8-wk-old ICOS$^{+/+}$ NOD mice ($n = 6$). Plots show representative staining of ICOS intensity gated on CD4$^+$ living cells. Numbers represent the percentage of ICOS$^+$ cells within CD4$^+$. Data are representative of three independent experiments. (B) ICOS expression during T1D development. Expression of ICOS on unmanipulated T cells from spleen, PLN, ALN, pancreas of 3, 5, and 8-wk-old ICOS$^{+/+}$ NOD mice ($n = 6$ *per* group). Each bar corresponds to the mean ± SD of values obtained. *$p<0.05$ (Student's *t*-test). Data are representative of three independent experiments. (C) β cells do not express ICOSL. The first dot plot on the left shows how β cells were distinguished from non-β cells based on their autofluorescence (FAD content) and cell size, resulting in a population with 90% (insulin-positive) β cells. Second and third dot plots on the right show representative staining of ICOSL intensity gated on unmanipulated β cells pooled from three pancreas of 8-wk-old ICOS$^{+/+}$ or ICOS$^{-/-}$ NOD mice. Numbers are percentage of ICOSL$^+$ cells within insulin-positive β cells. As positive control, the lower dot plot shows representative staining of ICOSL intensity gated on unmanipulated CD19$^+$ cells pooled from ALN from 8-wk-old ICOS$^{+/+}$ NOD mice, treated as β cells with collagenase and dissociation buffer. Data representative of five independent experiments.

T1D in BDC2.5 ICOS$^{-/-}$ NOD mice as compared with BDC2.5 ICOS$^{+/+}$ NOD mice (Fig. 3A). At 20 wk of age, 66% of female BDC2.5 ICOS$^{-/-}$ became diabetic, as compared with 8.33% of

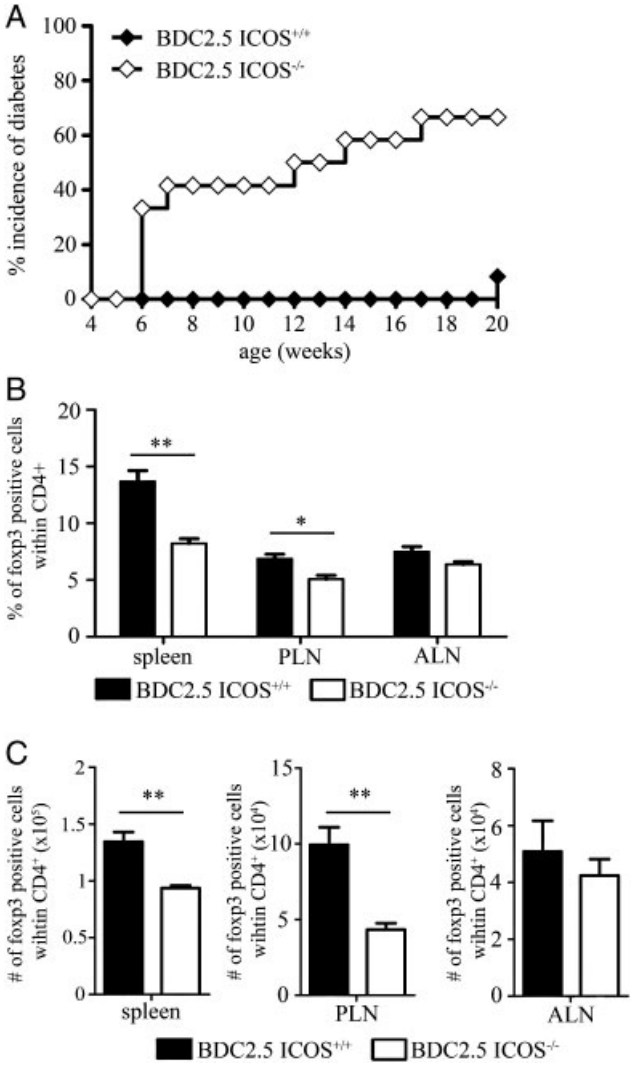

Figure 3. Acute T1D and decreased Treg in spleen and PLN of BDC2.5 ICOS$^{-/-}$ NOD mice. (A) BDC2.5 ICOS$^{-/-}$ NOD mice develop acute T1D. Spontaneous incidence of T1D in BDC2.5 ICOS$^{+/+}$ (♦, $n = 10$ mice) and BDC2.5 ICOS$^{-/-}$ (◇, $n = 10$ mice) NOD females. *p<0.05 (Logrank Test). (B, C) Decreased Treg in BDC2.5 ICOS$^{-/-}$ NOD mice. Percentage (B) and absolute number (C) of Foxp3$^+$ cells within CD4$^+$ T cells in spleen, PLN, ALN of 8-wk-old, unmanipulated, BDC2.5 ICOS$^{+/+}$ ($n = 7$) or BDC2.5 ICOS$^{-/-}$ ($n = 8$) NOD mice. Each bar represents the mean ± SD of values obtained. *p<0.05 and **p<0.01 (Student's t-test). Data representative of three independent experiments.

control mice. This observation raises the possibility that the ICOS pathway may control both the activation of autoimmune T_{eff} cells and of Treg, but that T-cell dependence on ICOS may vary depending on the T-cell clone considered.

A significant decrease in the absolute number and the percentage of CD4$^+$Foxp3$^+$ T cells was observed in spleen and PLN obtained from BDC2.5 ICOS$^{-/-}$ NOD mice as compared with WT littermates (Fig. 3B and C). A 26.3–40.0% decrease of percentages of CD4$^+$Foxp3$^+$ T cells was observed in BDC2.5 ICOS$^{-/-}$ NOD mice, respectively, in PLN and spleen. Considering absolute numbers of CD4$^+$Foxp3$^+$ T cells, a comparable decrease was observed, with a 31–48% decreased in spleen and PLN. Similar results were obtained in ICOS$^{-/-}$ and ICOSL$^{-/-}$ NOD mice as compared with their respective littermates (Supporting Information Fig. 1). Whatever the strains considered, no decrease was seen in ALN.

We next evaluated the ability of Treg from BDC2.5 ICOS$^{-/-}$ NOD mice, as compared with control cells, to inhibit the proliferative response of T_{eff} cells to anti-CD3 Ab or RVRPLWVRME mimotope peptide. As shown in Fig. 4A, no defective inhibitory capacity of CD4$^+$CD25$^+$ Treg from BDC2.5 ICOS$^{-/-}$ NOD mice was observed when cells were stimulated with anti-CD3 Ab. In contrast, CD4$^+$CD25$^+$ Treg from BDC2.5 ICOS$^{-/-}$ NOD mice were less efficient in suppressing the proliferative response of CD4$^+$CD25$^-$ T_{eff} cells from BDC2.5 ICOS$^{+/+}$ NOD mice to stimulation by the RVRPLWVRME peptide than BDC2.5 CD4$^+$CD25$^+$ Treg from BDC2.5 ICOS$^{+/+}$ NOD mice (Fig. 4B). These results were confirmed at various CD4$^+$CD25$^+$/CD4$^+$CD25$^-$ T-cell ratios. Taken together, our data suggest that qualitative and quantitative defects in ICOS-dependent Treg drive the increased incidence of T1D in transgenic BDC2.5 ICOS$^{-/-}$ NOD mice.

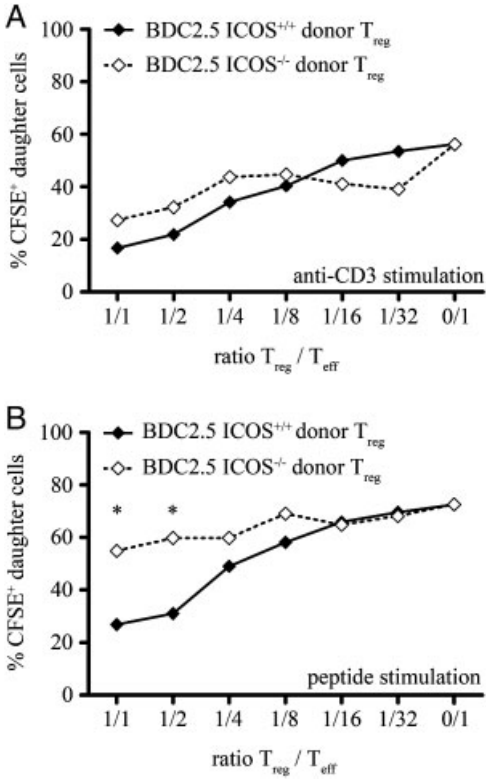

Figure 4. Treg from BDC2.5 ICOS$^{-/-}$ are less efficient in suppressing T-cell proliferation in response to peptide stimulation. (A, B) In total, 5×10^4 CD4$^+$CD25$^-$CFSE$^+$ T_{eff} cells (T_{eff} cells) from 8-wk-old BDC2.5 ICOS$^{+/+}$ NOD mice ($n = 3$) were cultured in the presence of CD4$^+$CD25$^+$ Treg from 8-wk-old BDC2.5 ICOS$^{+/+}$ (♦ BDC2.5 ICOS$^{+/+}$ donor Treg, $n = 3$) or BDC2.5 ICOS$^{-/-}$ (◇ BDC2.5 ICOS$^{-/-}$ donor Treg, $n = 3$) NOD mice at indicated ratio (T_{reg}/T_{eff}). Cells were stimulated by anti-CD3 Ab (1 μg/mL, (A)) or by RVRPLWVRME peptide (60 μg/mL, (B)). Proliferation of CD4$^+$CD25$^-$ T_{eff} cells was assessed after 72h by CFSE dilution. *p<0.05 (Student's t-test). Data are representative of three independent experiments.

A low frequency of ICOS-independent diabetogenic precursors contributes to diabetes protection in ICOS$^{-/-}$ NOD mice

The development of accelerated T1D in BDC2.5 ICOS$^{-/-}$ NOD mice points to diabetogenic BDC2.5 T_{eff} cells as ICOS-independent. The difference between polyclonal T cells in conventional NOD mice and BDC2.5 T cells in BDC2.5 transgenics is likely in the frequency of corresponding precursors. To test this hypothesis, we performed transfer experiments in which an increasing ratio of BDC2.5 monoclonal T_{eff} cells/polyclonal T_{eff} cells was transferred into ICOSL$^{-/-}$ NOD.*scid* recipients. As shown in Fig. 5, 2×10^5 CD4$^+$CD25$^-$ T_{eff} cells from ICOS$^{-/-}$ NOD mice failed to transfer T1D, as it was the case when 1×10^3 CD4$^+$ CD25$^-$ T_{eff} cells from BDC2.5 ICOS$^{-/-}$ mice and 1.99×10^5 CD4$^+$ CD25$^-$ polyclonal T_{eff} cells from conventional ICOS$^{-/-}$ NOD mice were cotransfered into ICOSL$^{-/-}$ NOD.*scid* recipients (ratio 1:100). In contrast, co-injection of 5×10^3 CD4$^+$CD25$^-$ T_{eff} cells from BDC2.5 ICOS$^{-/-}$ NOD mice with 1.95×10^5 CD4$^+$CD25$^-$ T_{eff} cells from ICOS$^{-/-}$ NOD mice (ratio 1:40) was sufficient to efficiently transfer T1D in ICOSL$^{-/-}$ NOD.*scid* recipients. The frequency of potent diabetogenic T_{eff} cells thus explains the opposite T1D phenotype observed in conventional ICOS$^{-/-}$ NOD mice and BDC2.5 ICOS$^{-/-}$ NOD mice.

Development of neuromuscular autoimmunity in ICOS$^{-/-}$ and ICOSL$^{-/-}$ NOD mice

Beginning at 20 wk of age, ICOS$^{-/-}$ and ICOSL$^{-/-}$ NOD mice exhibited a symmetrical, rapidly progressing hind leg paralysis with a higher prevalence in female (100 and 72.9%, respectively at 40 wk of age) than in males (20 and 26.9%, respectively, at 40 wk of age) (Fig. 6A). The disease was not observed in

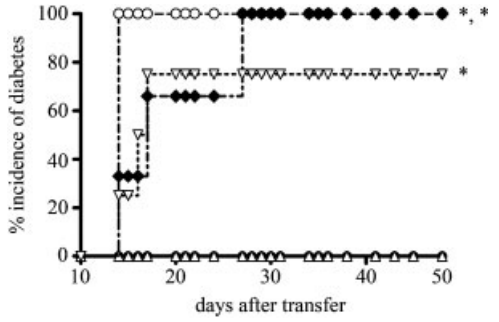

Figure 5. Dependence of NOD diabetogenic T cells on the ICOS pathway is determined by frequency of precursors. About 8-wk-old ICOSL$^{-/-}$ NOD.*scid* mice were injected with CD4$^+$CD25$^-$ T_{eff} cells from 14-wk-old ICOS$^{-/-}$ NOD mice (ICOS$^{-/-}$ donor T_{eff}) and/or from BDC2.5 ICOS$^{-/-}$ NOD mice (BDC2.5 ICOS$^{-/-}$ donor T_{eff}) at indicated ratio (● 2×10^5 ICOS$^{-/-}$ donor T_{eff}, $n = 3$; △ 1.99×10^5 ICOS$^{-/-}$ donor T_{eff} and 1×10^3 BDC2.5 ICOS$^{-/-}$ donor T_{eff}, $n = 4$; ▽ 1.95×10^5 ICOS$^{-/-}$ donor T_{eff} and 5×10^3 BDC2.5 ICOS$^{-/-}$ donor T_{eff}, $n = 4$; ◆ 1.90×10^5 ICOS$^{-/-}$ donor T_{eff} and 1×10^4 BDC2.5 ICOS$^{-/-}$ donor T_{eff}, $n = 4$; ○ 2×10^5 BDC2.5 ICOS$^{-/-}$ donor T_{eff}, $n = 3$). *$p<0.05$ as compared with mice injected with 2×10^5 ICOS$^{-/-}$ donor T_{eff} (Logrank Test). Data are representative of three independent experiments.

corresponding control NOD mice. ICOS$^{-/-}$ NOD mice showing evidence for paralysis were analyzed for pathological alterations in the nervous system and muscle (Fig. 6B). Inflammatory infiltrates seen in muscles, peripheral nerves, sensory ganglia, brain, and spinal cord were composed of T cell, macrophages, and a variable number of granulocytes. Overall, the picture was that of a T-cell-mediated inflammatory reaction, potentially of autoimmune origin. By contrast, no histological lesions were seen in control ICOS$^{+/+}$ NOD mice in the corresponding organs (Fig. 6B).

To assess whether muscular and neurological lesions were immune-mediated, purified T cells including CD4$^+$ T cells and CD8$^+$ T cells, splenocytes depleted of CD4$^+$ and CD8$^+$ T cells or total splenocytes from 40-wk-old ICOS$^{-/-}$ or ICOS$^{+/+}$ NOD mice were first activated *in vitro*, then adoptively transferred into conventional NOD.*scid* recipients (Fig. 6C). Muscular and neurological symptoms, consisting in hind leg weakness and ataxia, were observed only in recipients of total splenocytes or purified T cells including CD4$^+$ and CD8$^+$ T cells from ICOS$^{-/-}$ NOD mice. Clinical paralysis started 4–6 wk post-transfer. In contrast, none of the NOD.*scid* recipients that received total splenocytes or purified T cells including CD4$^+$ and CD8$^+$ T cells from ICOS$^{-/-}$ NOD mice developed T1D. Clinical T1D was observed only in recipient mice transferred with corresponding T cells from ICOS$^{+/+}$ NOD mice (data not shown). Neither T1D nor neuromuscular disease was observed in mice transferred by splenocytes depleted of both CD4$^+$ and CD8$^+$ T cells from ICOS$^{+/+}$ or ICOS$^{-/-}$ NOD mice. Histological analyses of recipient mice were performed 30 days after transfer. Although no infiltrates were found in CNS, the same pathological alterations as those seen in ICOS$^{-/-}$ mice developing a spontaneous neuromuscular disease were observed in the peripheral nervous system (PNS) and in muscles (data not shown).

Since a similar neuropathy phenotype was previously reported in the B7.2$^{-/-}$ NOD mice, and since the ICOS/ICOSL costimulation pathway belongs to the same costimulation superfamily as CD28/B7, we checked the expression of CD28, B7, and CTLA-4. No significant difference in the expression of CD28 and CTLA-4 on T cells was seen in ICOS$^{-/-}$ NOD mice as compared with ICOS$^{+/+}$ NOD mice (data not shown). As shown in Fig. 6D, expression of B7.1 and B7.2 on B cells remains unchanged in both strains before and after 24 h stimulation by LPS. These data demonstrate that the neuropathy observed in ICOS$^{-/-}$ NOD mice does not depend on secondary modifications of the CD28/B7 pathway.

Discussion

Given the role of costimulation in T-cell responses to antigens, attempts to modulate signaling through costimulatory pathways are expected to modify the development of autoimmunity in models in which T cells are central in the autoimmune process [13, 14, 23]. Understanding the role of the ICOS/ICOSL costimulatory pathway in processes that lead to autoimmune destruction of pancreatic β cells in T1D is thus a key issue and the

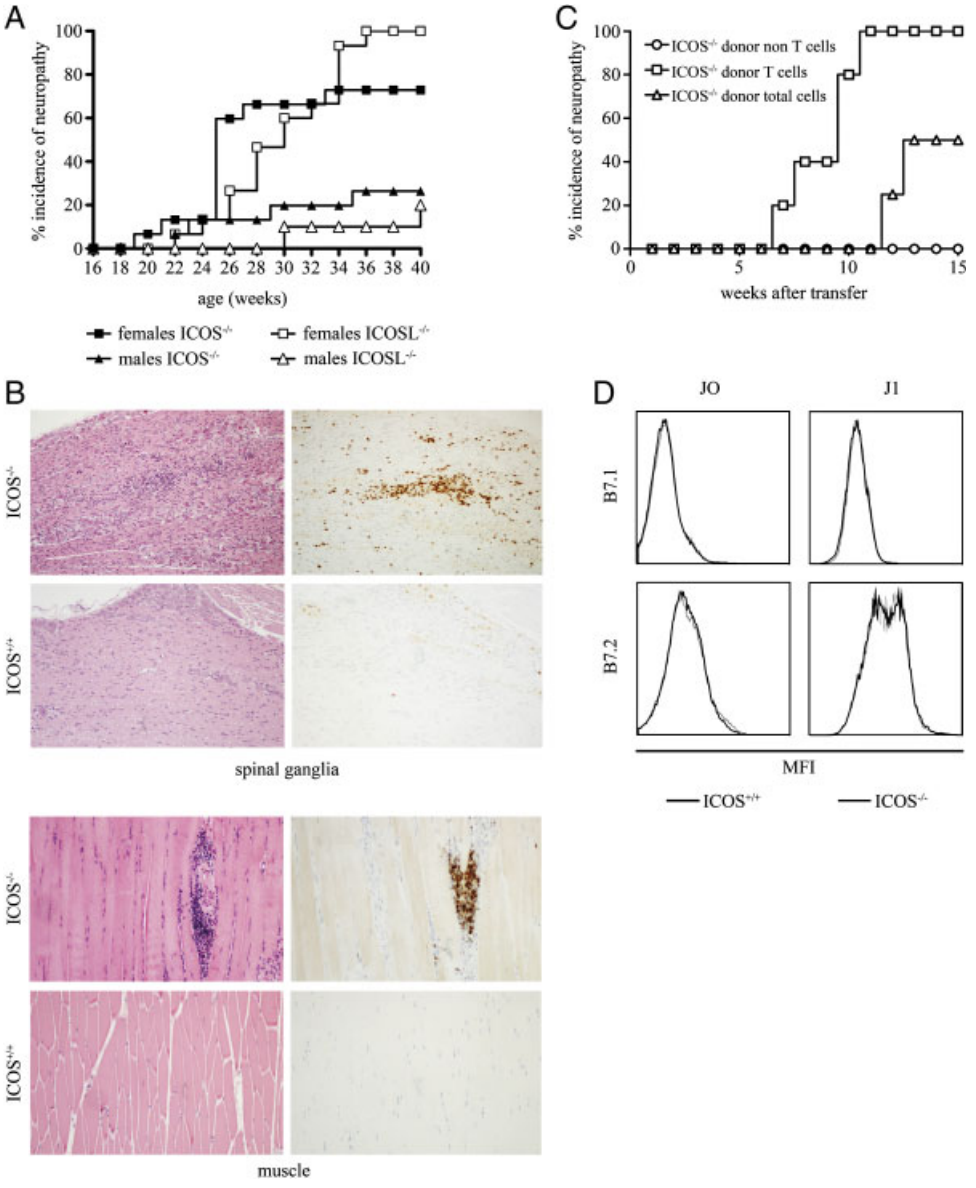

Figure 6. Muscle and neural autoimmunity in ICOS$^{-/-}$ NOD mice. (A) Spontaneous incidence of neuropathy in male (▲, $n = 10$) and female (■, $n = 10$) ICOS$^{-/-}$ NOD mice and in male (△, $n = 15$) and female (□, $n = 15$) ICOSL$^{-/-}$ NOD mice. Mice were checked weekly for clinical signs of neuropathy, consisting chronologically in hind legs weakness, ataxia, and sensitive troubles. Data are representative of two independent experiments. (B) Histology of spinal ganglia and muscles from 40-wk-old ICOS$^{+/+}$ or ICOS$^{-/-}$ NOD females. As compared with age-matched female ICOS$^{+/+}$ NOD mice, female ICOS$^{-/-}$ NOD mice show inflammation and infiltrating T cells (left column for hematoxylin and eosin staining, 90 × magnification; right column for anti-CD3 immunocytochemistry staining, 90 × magnification) in spinal ganglia (upper panel) and in muscle (lower panel). (C) Briefly, 8-wk-old NOD.*scid* mice ($n = 5$ *per* group) were injected with 10×10^6 stimulated total spleen cells (△, ICOS$^{-/-}$ donor total cells), 5×10^6 purified stimulated T cells including CD4$^+$ T cells and CD8$^+$ T cells (□, ICOS$^{-/-}$ donor T cells), 5×10^6 stimulated splenocytes depleted of CD4$^+$ and CD8$^+$ T cells (○, ICOS$^{-/-}$ donor non-T cells) from 40-wk-old ICOS$^{-/-}$ NOD mice. Data are representative of three independent experiments. (D) The CD28/B7 pathway is not altered in the ICOS$^{-/-}$ NOD mice. Flow cytometric analysis of B7.1 and B7.2 expression on B cells from spleen of 8-wk-old ICOS$^{+/+}$ or ICOS$^{-/-}$ NOD mice before and after *in vitro* stimulation by LPS. Plots show representative staining of B7.1 or B7.2 intensity gated on CD19$^+$ living cells. Data are representative of three independent experiments.

first step toward potential therapeutic applications. In this study, using a genetic deletion approach, we have demonstrated that the ICOS/ICOSL costimulation pathway is required for the development of T1D in the NOD mouse. We observed that ICOS$^{-/-}$ and, for the first time, ICOSL$^{-/-}$ NOD mice are both protected from developing T1D. Since the *Icos* gene and the *Icosl* gene locate on different chromosomes, our data indicate that protection against T1D directly relates with deficient ICOS/ICOSL pathway and is not due to the effect of a distinct *Idd* gene located in the vicinity of *Icos*, such as *Cd28* [6, 7] or *Ctla4* [8]. Moreover, the inefficiency of cyclophosphamide injections to induce acute T1D, the striking protection from insulitis in 40-wk-old ICOS$^{-/-}$, and ICOSL$^{-/-}$ NOD mice, the failure to transfer T1D into NOD.*scid* mice after adoptive transfer of splenocytes from

ICOS$^{-/-}$ NOD mice suggests that the ICOS/ICOSL pathway is necessary in the early steps that lead to the failure of immune tolerance to β cells.

Interestingly, as compared with the levels of expression within spleen, PLN, and ALN, a high percentage of islet-infiltrating CD4$^+$ T cells express ICOS in conventional 8-wk-old NOD mice. More surprisingly, no peak of ICOS expression was ever observed in PLN along T1D development. However, it is possible that we failed to capture an ICOS expression peak since activated T cells rapidly migrate into the islets where further increase in ICOS expression is likely to take place. We studied ICOSL expression in pancreas in order to further precise the role of the ICOS/ICOSL pathway in the islets. *In situ*, ICOSL expression was restricted to conventional APC. No ICOSL expression was observed on β cells. High ICOS expression by islet T cells is thus possibly secondary to the local expansion of diabetogenic T cells within the islets independently of ICOSL expression by β cells.

Although we cannot exclude that the ICOS/ICOSL pathway is necessary for activation and homeostasis of diabetogenic T cells, we have to take into account the role of ICOS and ICOSL in T-cell-dependent B-cell responses [22, 24–26]. The ICOS/ICOSL pathway is indeed critical for isotypic commutation and somatic mutation in B cells. Defective *Icos* or *Icosl* expression in NOD mice is expected to disrupt interactions between T and B cells and prevent the failure of immune tolerance to β cells initiated by B lymphocytes. B cells are essential APC during T1D development [27–29]. This is consistent with the diminished production of auto-Ab that has been previously reported in ICOS$^{-/-}$ NOD mice [20].

The increased incidence of T1D seen in BDC2.5 ICOS$^{-/-}$ NOD mice suggests that the ICOS/ICOSL pathway is critical for Treg. In ICOS$^{-/-}$ and BDC2.5 ICOS$^{-/-}$ NOD mice, a significant decrease in percent and absolute number of CD4$^+$Foxp3$^+$ T cells is seen in spleen and PLN although not in ALN. This difference may reflect the local immune activation process that leads to T1D. Interestingly, *in vitro*, CD4$^+$CD25$^+$ Treg from BDC2.5 ICOS$^{-/-}$ NOD mice were significantly less efficient than control Treg in suppressing the T-cell response to a mimitope peptide but not to anti-CD3 Ab. These observations suggest that the ICOS/ICOSL pathway is critical for the function of both T_{eff} cells and Treg, but that the dependence of T cells on ICOS varies depending on the T-cell clone considered and the strength of signals involved in T-cell activation.

Accelerated T1D in ICOS$^{-/-}$ BDC2.5 NOD mice indicates that all diabetogenic T_{eff} cells do not depend on the ICOS/ICOSL costimulation pathway. Affinity of the TCR for peptide–major histocompatibility complexes is expected to inversely correlate with dependence of T-cell activation on ICOS costimulation. Addressing the affinity issue would require studying transgenic mice carrying different TCR specific for the same peptide–major histocompatibility complexes. However, transfer experiments using decreasing dilution of BDC2.5 diabetogenic T_{eff} cells in a polyclonal NOD T_{eff} cells pool allowed showing that the frequency of ICOS-independent diabetogenic T_{eff} explains the opposite T1D phenotype observed in conventional ICOS$^{-/-}$ NOD mice and BDC2.5 ICOS$^{-/-}$ NOD mice.

For the first time, we report, in both ICOS$^{-/-}$ and ICOSL$^{-/-}$ NOD mice, a deviation of autoimmunity from the islets toward muscles, peripheral nerves, sensory ganglia, and, to a lesser extent, the CNS. Diffuse inflammatory infiltrates composed of T cells, macrophages, and variable numbers of granulocytes are observed, similar to those seen in autoimmune encephalitis, neuritis, and myositis. The observation of muscle and peripheral nerve autoimmunity is not unexpected if one considers that, beyond spontaneously developing T1D, NOD mice are susceptible to many other autoimmune diseases. These include autoimmune sialadenitis [30], autoimmune thyroiditis [31], hemolytic anemia [32], and prostatitis in male mice [33]. Accordingly, the NOD-derived mouse has been considered as a model of primary Sjogren syndrome, Guillain-Barré syndrome and multiple sclerosis [34–36].

A shift from T1D to other autoimmune diseases has been evidenced in NOD mice in which a costimulatory molecule that is distinct from ICOSL, B7.2, was disrupted [34]. Autoimmunity in B7.2$^{-/-}$ NOD mice is directed against myelin protein zero and is mainly directed against the PNS [37]. A critical point is that the CD28/B7 pathway remains unaltered in ICOS$^{-/-}$ NOD mice as compared with control mice. Moreover, autoimmune deviation in ICOS$^{-/-}$ NOD mice extends to muscles, sensory ganglia and to a lower extent the CNS while it is only restricted to PNS in B7.2$^{-/-}$ NOD mice. Our observation, along with the previous report in the B7.2$^{-/-}$ NOD model, points to local interactions of T cells with other cell partners as a key factor in maintenance or disruption of organ-specific immune tolerance. Further experiments will be required to address whether T_{eff} cells that drive muscle and/or neurological autoimmunity in ICOS$^{-/-}$ NOD mice can be down-regulated by Treg from ICOS$^{+/+}$ NOD mice that are likely to be ICOS-independent.

In conclusion, we bring evidence that ICOS/ICOSL interaction controls in part the activation of diabetogenic T_{eff} cells and influences the balance between Treg and diabetogenic T_{eff} cells. This likely explains the discordant observations made in conventional and transgenic BDC2.5 NOD mice. Furthermore, although ICOS$^{-/-}$ or ICOSL$^{-/-}$ NOD mice are protected from T1D, they develop autoimmunity against neural and muscular tissues, indicating that ICOS–ICOSL interactions are important in polarizing the NOD autoimmune response.

Materials and methods

Mice

NOD, ICOS$^{-/-}$ NOD, ICOSL$^{-/-}$ NOD, NOD.*scid*, ICOSL$^{-/-}$ NOD.*scid*, BDC2.5 NOD and BDC2.5 ICOS$^{-/-}$ NOD mice were bred and housed in our facilities under specific pathogen-free conditions. ICOS$^{-/-}$ NOD mice were generated by crossing NOD mice with ICOS$^{-/-}$ [22] and backcrossing for nine generations to NOD mice. ICOSL$^{-/-}$ NOD mice were generated by backcrossing ICOSL$^{-/-}$ [38] to NOD mice for 16 generations. The prevalence

of T1D in our NOD colony reaches 10% in males and 75% in females by 6 month of age. Animal studies were approved by institutional review.

Diabetes assessments

T1D was assessed by monitoring mice for glycosuria using test strips from 4 wk on twice a week for spontaneous incidence or three times a week, 10 days after the beginning of adoptive transfer experiments. Blood glucose was measured (Euroflash, Lifescan, Milpitas, CA) when glycosuria was detected. Mice were diagnosed as diabetic after two consecutive glycemia over 200 mg/dL. The onset of T1D was dated from the first of the sequential glycemia measurements.

Histological analysis

To evaluate inflammation in nervous tissue and muscle, animals were perfused, fixed by 4% formaldehyde solution (Electron Microscopy Science, Hatfield, PA), then spinal ganglia and pieces of different skeletal muscles were dissected and embedded into paraffin. Briefly, 3 m sections were stained with hematoxylin and eosin. Immunocytochemistry was performed with primary Ab against T cells (CD3; MCA 1477; Serotec, GB) using a biotin/avidin/peroxidase technique.

Flow cytometric analysis

Ab

The following mAb were used (hybridoma clone indicated in parentheses): PerCP-anti-CD4 (RM4-5), PE-anti-ICOSL (HK5.3) from BD Bioscience (San Jose, CA); FITC-anti-B7.1 (16–10A1), PE-anti-B7.2 (GL1), APC-anti-CD19 (MB19-1), Biotine-anti-CD278/ICOS (15F9), PE-anti-Foxp3 (FJK-16s) from eBioscience (San Diego, CA). β cells were stained with bovin anti-insulin Ab (Sigma-Aldrich, St. Louis, MO) then with Biotin-SP-AffiniPure Goat Anti-Guinea Pig IgG (Jakson Immunoresearch Laboratories, West Grove, PA). Appropriate isotype control mAb were included.

Immunofluorescence staining

Single-cell suspensions were pelleted in 96-well plates, preincubated with 10 μg/mL 2.4G2 for 15 min at 4°C and washed twice in order to minimize unspecific binding. Cells were then stained for 30 min at 4°C with optimal concentrations of reagents in 20 μL of PBS supplemented with 2% FBS and 5 mM sodium azide. Cells were washed twice, stained again if necessary, or resuspended in PBS containing 1% formaldehyde. Intracellular Foxp3 staining was performed according to the manufacturer's instructions (Foxp3 anti-mouse/rat Foxp3 staining set; eBioscience). Flow cytometric analysis was performed using a FACSCalibur, FlowJo softwares (Tree Star, Ashland, OR).

Cell purifications

$CD4^+CD25^-$ and $CD4^+CD25^+$ T cells were purified through a first step of $CD4^+$ T-cell enrichment using mouse $CD4^-$ Selection Kit (Invitrogen Dynal AS, Carlsbad, CA) according to the manufacturer's instructions. Cells were then separated by MACS sorting, using LS columns, biotin-anti-CD25 (7D4, BD Bioscience) Ab, and streptavidin beads according to the manufacturer's instructions (Miltenyi Biotec, Bergisch Gladbach, Germany): $CD4^+CD25^+$ T cells were recovered from the "positive" fraction, whereas $CD4^+CD25^-$ T cells were in the flow through. Purified T cells including $CD4^+$ T cells and $CD8^+$ T cells, splenocytes depleted of $CD4^+$ and $CD8^+$ T cells were directly separated by MACS sorting as described above using biotin-anti-CD8 and biotin-anti-CD4 Ab prepared in the laboratory. β cells were prepared using collagenase as described previously [39] with slight modifications and further digestion in enzyme-free cell-dissociation buffer (Invitrogen).

In vitro suppression assay

$CD4^+CD25^+$ and $CD4^+CD25^-$ T cells were sorted as described above from pooled spleen cells of three 8-wk-old BDC2.5 $ICOS^{+/+}$ or BDC2.5 $ICOS^{-/-}$ NOD mice. $CD4^+CD25^-$ T_{eff} cells from BDC2.5 $ICOS^{+/+}$ NOD mice were labeled by incubation with 5 μM CFSE (Molecular Probes, Invitrogen) for 15 min at 37°C. Cells were then incubated in triplicate wells in 96-plates at 5×10^4/well with different ratios of unlabeled $CD4^+CD25^+$ Treg from BDC2.5 $ICOS^{+/+}$ or BDC2.5 $ICOS^{-/-}$ NOD mice. Cells were stimulated in the presence of anti-CD3 (1 μg/mL, eBioscience) or RVRPLWVRME peptide (60 μg/mL) and 1×10^5 irradiated $CD4^+$ and $CD8^+$-depleted splenocytes from BDC2.5 $ICOS^{-/-}$ NOD mice. Proliferation of CFSE-labeled $CD4^+CD25^-$ T_{eff} cells was assessed after 72h by flow cytometry.

Adoptive cell transfers

$CD4^+CD25^-$ T_{eff} cells, purified T cells including $CD4^+$ T cells and $CD8^+$ T cells, splenocytes depleted of $CD4^+$, and $CD8^+$ T cells from 8, 14, or 40-wk-old either $ICOS^{+/+}$, $ICOS^{-/-}$, BDC2.5 $ICOS^{+/+}$, BDC2.5 $ICOS^{-/-}$ NOD mice were sorted as described above. When indicated, cells were stimulated with 1 μg/mL anti-CD3 (BD Bioscience) and anti-CD28 (BD Bioscience) for 48 h. IL2 (20 U/mL, R&D Systems, Minneapolis, MN) was added to the culture of the splenocytes depleted of $CD4^+$ and $CD8^+$ T cells. Total spleen cells or purified T cells, stimulated or not, were then adoptively transferred as indicated in figure legends i.v. into 8-wk-old $ICOSL^{+/+}$ or $ICOSL^{-/-}$ NOD.*scid* mice as described previously [40].

Ten days after the transfer, mice were evaluated three times a week, for clinical T1D or neuropathy (consisting in hind legs weakness, ataxia) during 15 wk or sacrificed 30 days after transfer, perfused, and fixed by 4% formaldehyde solution (Electron Microscopy Science) in order to perform histological analysis.

Statistical analysis

Appropriate statistical tests were performed on all data as indicated in figure legends using GraphPad Prism Version 4.0b software (GraphPad Software, La Jola, CA).

Acknowledgements: A. T. was supported by an "Avenir" INSERM contract. E. R. was supported by an FRM contract. C. B. was supported by INSERM contract.

Conflict of interest: The authors declare no financial or commercial conflict of interest.

References

1 **Faideau, B., Larger, E., Lepault, F., Carel, J. C. and Boitard, C.,** Role of beta-cells in type 1 diabetes pathogenesis. *Diabetes* 2005. **54**: S87–S96.

2 **Anderson, M. S. and Bluestone, J. A.,** The NOD mouse: a model of immune dysregulation. *Annu. Rev. Immunol.* 2005. **23**: 447–485.

3 **Jones, E. Y., Fugger, L., Strominger, J. L. and Siebold, C.,** MHC class II proteins and disease: a structural perspective. *Nat. Rev. Immunol.* 2006. **6**: 271–282.

4 **Toma, A., Haddouk, S., Briand, J. P., Camoin, L., Gahery, H., Connan, F., Dubois-Laforgue, D. *et al.*,** Recognition of a subregion of human proinsulin by class I-restricted T cells in type 1 diabetic patients. *Proc. Natl. Acad. Sci. USA* 2005. **102**: 10581–10586.

5 **Wong, F. S., Visintin, I., Wen, L., Flavell, R. A. and Janeway, C. A., Jr.,** CD8 T cell clones from young nonobese diabetic (NOD) islets can transfer rapid onset of diabetes in NOD mice in the absence of CD4 cells. *J. Exp. Med.* 1996. **183**: 67–76.

6 **Hara, T., Fu, S. M. and Hansen, J. A.,** Human T cell activation. II. A new activation pathway used by a major T cell population *via* a disulfide-bonded dimer of a 44 kilodalton polypeptide (9.3 antigen). *J. Exp. Med.* 1985. **161**: 1513–1524.

7 **Gross, J. A., St John, T. and Allison, J. P.,** The murine homologue of the T lymphocyte antigen CD28. Molecular cloning and cell surface expression. *J. Immunol.* 1990. **144**: 3201–3210.

8 **Brunet, J. F., Denizot, F., Luciani, M. F., Roux-Dosseto, M., Suzan, M., Mattei, M. G. and Golstein, P.,** A new member of the immunoglobulin superfamily – CTLA-4. *Nature* 1987. **328**: 267–270.

9 **Yoshinaga, S. K., Whoriskey, J. S., Khare, S. D., Sarmiento, U., Guo, J., Horan, T., Shih, G. *et al.*,** T-cell co-stimulation through B7RP-1 and ICOS. *Nature* 1999. **402**: 827–832.

10 **Hutloff, A., Dittrich, A. M., Beier, K. C., Eljaschewitsch, B., Kraft, R., Anagnostopoulos, I. and Kroczek, R. A.,** ICOS is an inducible T-cell co-stimulator structurally and functionally related to CD28. *Nature* 1999. **397**: 263–266.

11 **Todd, J. A. and Wicker, L. S.,** Genetic protection from the inflammatory disease type 1 diabetes in humans and animal models. *Immunity* 2001. **15**: 387–395.

12 **Ueda, H., Howson, J. M., Esposito, L., Heward, J., Snook, H., Chamberlain, G., Rainbow, D. B. *et al.*,** Association of the T-cell regulatory gene CTLA4 with susceptibility to autoimmune disease. *Nature* 2003. **423**: 506–511.

13 **Lenschow, D. J., Ho, S. C., Sattar, H., Rhee, L., Gray, G., Nabavi, N., Herold, K. C. *et al.*,** Differential effects of anti-B7-1 and anti-B7-2 monoclonal antibody treatment on the development of diabetes in the nonobese diabetic mouse. *J. Exp. Med.* 1995. **181**: 1145–1155.

14 **Lenschow, D. J., Herold, K. C., Rhee, L., Patel, B., Koons, A., Qin, H. Y., Fuchs, E. *et al.*,** CD28/B7 regulation of Th1 and Th2 subsets in the development of autoimmune diabetes. *Immunity* 1996. **5**: 285–293.

15 **Salomon, B., Lenschow, D. J., Rhee, L., Ashourian, N., Singh, B., Sharpe, A. and Bluestone, J. A.,** B7/CD28 costimulation is essential for the homeostasis of the CD4+CD25+ immunoregulatory T cells that control autoimmune diabetes. *Immunity* 2000. **12**: 431–440.

16 **Luhder, F., Hoglund, P., Allison, J. P., Benoist, C. and Mathis, D.,** Cytotoxic T lymphocyte-associated antigen 4 (CTLA-4) regulates the unfolding of autoimmune diabetes. *J. Exp. Med.* 1998. **187**: 427–432.

17 **Ansari, M. J., Salama, A. D., Chitnis, T., Smith, R. N., Yagita, H., Akiba, H., Yamazaki, T. *et al.*,** The programmed death-1 (PD-1) pathway regulates autoimmune diabetes in nonobese diabetic (NOD) mice. *J. Exp. Med.* 2003. **198**: 63–69.

18 **Ansari, M. J., Fiorina, P., Dada, S., Guleria, I., Ueno, T., Yuan, X., Trikudanathan, S. *et al.*,** Role of ICOS pathway in autoimmune and alloimmune responses in NOD mice. *Clin. Immunol.* 2008. **126**: 140–147.

19 **Nanji, S. A., Hancock, W. W., Luo, B., Schur, C. D., Pawlick, R. L., Zhu, L. F., Anderson, C. C. *et al.*,** Costimulation blockade of both inducible costimulator and CD40 ligand induces dominant tolerance to islet allografts and prevents spontaneous autoimmune diabetes in the NOD mouse. *Diabetes* 2006. **55**: 27–33.

20 **Hawiger, D., Tran, E., Du, W., Booth, C. J., Wen, L., Dong, C. and Flavell, R. A.,** ICOS mediates the development of insulin-dependent diabetes mellitus in nonobese diabetic mice. *J. Immunol.* 2008. **180**: 3140–3147.

21 **Herman, A. E., Freeman, G. J., Mathis, D. and Benoist, C.,** CD4+CD25+ T regulatory cells dependent on ICOS promote regulation of effector cells in the prediabetic lesion. *J. Exp. Med.* 2004. **199**: 1479–1489.

22 **Tafuri, A., Shahinian, A., Bladt, F., Yoshinaga, S. K., Jordana, M., Wakeham, A., Boucher, L. M. *et al.*,** ICOS is essential for effective T-helper-cell responses. *Nature* 2001. **409**: 105–109.

23 **Rottman, J. B., Smith, T., Tonra, J. R., Ganley, K., Bloom, T., Silva, R., Pierce, B. *et al.*,** The costimulatory molecule ICOS plays an important role in the immunopathogenesis of EAE. *Nat. Immunol.* 2001. **2**: 605–611.

24 **Dong, C., Juedes, A. E., Temann, U. A., Shresta, S., Allison, J. P., Ruddle, N. H. and Flavell, R. A.,** ICOS co-stimulatory receptor is essential for T-cell activation and function. *Nature* 2001. **409**: 97–101.

25 **McAdam, A. J., Greenwald, R. J., Levin, M. A., Chernova, T., Malenkovich, N., Ling, V., Freeman, G. J. *et al.*,** ICOS is critical for CD40-mediated antibody class switching. *Nature* 2001. **409**: 102–105.

26 **Gigoux, M., Shang, J., Pak, Y., Xu, M., Choe, J., Mak, T. W. and Suh, W. K.,** Inducible costimulator promotes helper T-cell differentiation through phosphoinositide 3-kinase. *Proc. Natl. Acad. Sci. USA* 2009. **106**: 20371–20376.

27 **Serreze, D. V., Fleming, S. A., Chapman, H. D., Richard, S. D., Leiter, E. H. and Tisch, R. M.,** B lymphocytes are critical antigen-presenting cells for

the initiation of T cell-mediated autoimmune diabetes in nonobese diabetic mice. *J. Immunol.* 1998. **161**: 3912–3918.

28 **Noorchashm, H., Noorchashm, N., Kern, J., Rostami, S. Y., Barker, C. F. and Naji, A.,** B-cells are required for the initiation of insulitis and sialitis in nonobese diabetic mice. *Diabetes* 1997. **46**: 941–946.

29 **Serreze, D. V., Chapman, H. D., Varnum, D. S., Hanson, M. S., Reifsnyder, P. C., Richard, S. D., Fleming, S. A. *et al.*,** B lymphocytes are essential for the initiation of T cell-mediated autoimmune diabetes: analysis of a new "speed congenic" stock of NOD.Ig mu null mice. *J. Exp. Med.* 1996. **184**: 2049–2053.

30 **Hu, Y., Nakagawa, Y., Purushotham, K. R. and Humphreys-Beher, M. G.,** Functional changes in salivary glands of autoimmune disease-prone NOD mice. *Am. J. Physiol.* 1992. **263**: E607–E614.

31 **Many, M. C., Maniratunga, S. and Denef, J. F.,** The non-obese diabetic (NOD) mouse: an animal model for autoimmune thyroiditis. *Exp. Clin. Endocrinol. Diabetes* 1996. **104**: 17–20.

32 **Oldenborg, P. A., Gresham, H. D., Chen, Y., Izui, S. and Lindberg, F. P.,** Lethal autoimmune hemolytic anemia in CD47-deficient nonobese diabetic (NOD) mice. *Blood* 2002. **99**: 3500–3504.

33 **Rivero, V. E., Cailleau, C., Depiante-Depaoli, M., Riera, C. M. and Carnaud, C.,** Non-obese diabetic (NOD) mice are genetically susceptible to experimental autoimmune prostatitis (EAP). *J. Autoimmun.* 1998. **11**: 603–610.

34 **Salomon, B., Rhee, L., Bour-Jordan, H., Hsin, H., Montag, A., Soliven, B., Arcella, J. *et al.*,** Development of spontaneous autoimmune peripheral polyneuropathy in B7-2-deficient NOD mice. *J. Exp. Med.* 2001. **194**: 677–684.

35 **Robinson, C. P., Yamachika, S., Bounous, D. I., Brayer, J., Jonsson, R., Holmdahl, R., Peck, A. B. *et al.*,** A novel NOD-derived murine model of primary Sjogren's syndrome. *Arthritis Rheum.* 1998. **41**: 150–156.

36 **Girvin, A. M., Dal Canto, M. C., Rhee, L., Salomon, B., Sharpe, A., Bluestone, J. A. and Miller, S. D.,** A critical role for B7/CD28 costimulation in experimental autoimmune encephalomyelitis: a comparative study using costimulatory molecule-deficient mice and monoclonal antibody blockade. *J. Immunol.* 2000. **164**: 136–143.

37 **Louvet, C., Kabre, B. G., Davini, D. W., Martinier, N., Su, M. A., DeVoss, J. J., Rosenthal, W. L. *et al.*,** A novel myelin P0-specific T cell receptor transgenic mouse develops a fulminant autoimmune peripheral neuropathy. *J. Exp. Med.* 2009. **206**: 507–514.

38 **Mak, T. W., Shahinian, A., Yoshinaga, S. K., Wakeham, A., Boucher, L. M., Pintilie, M., Duncan, G. *et al.*,** Costimulation through the inducible costimulator ligand is essential for both T helper and B cell functions in T cell-dependent B cell responses. *Nat. Immunol.* 2003. **4**: 765–772.

39 **Halbout, P., Briand, J. P., Becourt, C., Muller, S. and Boitard, C.,** T cell response to preproinsulin I and II in the nonobese diabetic mouse. *J. Immunol.* 2002. **169**: 2436–2443.

40 **Boitard, C., Yasunami, R., Dardenne, M. and Bach, J. F.,** T cell-mediated inhibition of the transfer of autoimmune diabetes in NOD mice. *J. Exp. Med.* 1989. **169**: 1669–1680.

Abbreviations: **ALN:** axillary LN · **ICOSL:** ICOS ligand · **PLN:** pancreatic LN · **PNS:** peripheral nervous system · **T_{eff} cells:** effector T cells · **T1D:** type 1 diabetes

Full correspondence: Professor Christian Boitard, INSERM U561, Hôpital Saint Vincent de Paul, 82 Avenue Denfert Rochereau, 75014 Paris, France
Fax: +33-0-1-40-48-83-52
e-mail: Christian.boitard@htd.aphp.fr

Received: 18/2/2010
Revised: 28/4/2010
Accepted: 4/6/2010
Accepted article online: 11/6/2010

